Journal of Applied Polymer Science

Influence of the environment during a photodegradation of multilayer films

Simon Lewandowski,[1,2] Virginie Rejsek-Riba,[2] Alain Bernès,[1] Sophie Perraud,[3] Colette Lacabanne[1]

[1]Physique Des Polymères, Institut Carnot CIRIMAT, Université Paul Sabatier, 118 Route De Narbonne, Toulouse Cedex 9, 31062, France

[2]ONERA, The French Aerospace Lab-DESP, Toulouse Cedex 04, F-31055, France

[3]Centre National D'Etudes Spatiales, 18 Avenue Edouard Belin, Toulouse Cedex 9, 31401, France

Correspondence to: A. Bernès (E-mail: alain.bernes@univ-tlse3.fr)

ABSTRACT: The influence of different stratosphere parameters on the degradation of a multilayer film was investigated. The selected multilayer was a three polymeric layers film, a polyamide 6 film inserted between two poly(ethylene terephthalate) (PET) films. Samples were exposed for several ageing under ultraviolet radiations (filtered at 270 nm), varying the atmosphere at 55 mbar pressure (atm, atm + ozone, N_2, and $T = -55\,°C$ or $+23\,°C$). Evolution of it mechanical properties defined by uniaxial tractions, thermo-optical properties defined by spectrophotometry UV–vis-NIR, chemical properties defined by FTIR-ATR, and thermal and dielectric properties defined, respectively, by differential scanning calorimetry (DSC) and dynamical dielectric spectroscopy (DDS), were investigated. Our results showed that UV irradiation causes multilayer films degradations, that is, principally decrease of UV transmittance and stress and strain at break (−50%). An increase of the ageing temperature causes an acceleration of these degradations. Degradations principally occur on the PET side of the multilayer exposed to UV radiation. Moreover, the DDS analysis shows a plasticization effect of the primary mode in the polyamide 6 due to photo-oxidation. Oxygen diffusion is the principal element for this plasticization, indeed it not occurs in a nonoxidative environment (nitrogen), or at low ageing temperature (−55 °C). © 2016 Wiley Periodicals, Inc. J. Appl. Polym. Sci. **2016**, *133*, 44075.

KEYWORDS: ageing; degradation; polyamides; polyesters

Received 13 January 2016; accepted 12 June 2016
DOI: 10.1002/app.44075

INTRODUCTION

Commercial applications of polymer films continuously increase. Among many polymer films available for numerous applications, poly(ethylene terephthalate) (PET) is one of the main polymers used. In some case, PET properties, like mechanical strength and durability, are not sufficient for application requirements. This is particularly necessary when drastic specifications are required or when materials are used in extreme conditions. In these cases, utilization of multilayer films is one of the solutions to meet the prospected properties.[1]

For numerous applications, like packing or food containers, polymer films are widely used today for outdoor applications. Exposure of polymers to outdoors conditions causes many irreversible changes. It produces unwanted effects like yellowing, evolution of gas permeability and decrease in mechanical properties. These changes severely impair the integrity of the polymer film, and their useful lifetimes will tend to decrease under exposure to sunlight.[2–8] To understand the different phenomena, photodegradation of PET has been widely investigated, under ultraviolet (UV) irradiation in standard atmosphere, to reproduce daily utilization.[9–15] Radiations of low wavelength, the most energetic, are responsible for larger changes observed during exposure to the sun.[16] The impact of the presence of oxidative elements during the photodegradation was also studied by Day and Wiles, who highlighted the importance of oxidizing elements during ageing. Oxidative environment limits crosslinking by reacting with radicals created during the photoscission.[16,17]

The development and the utilization of multilayer films lead to the qualification necessity of these new materials. In a previous work, an investigation had been done on signals identification of the different films constituting the multilayer films studied and on its properties evolution during a one week ageing in an 1 atm pressure atmosphere.[18] Photodegradation of the first layer PET was observed. This degradation induces the decrease of mechanical properties at break and decrease in UV transmission for low wavelengths. With the dynamical dielectric spectroscopy (DDS), the inner layer was also studied. Plasticizing effect was detected, as a consequence of photodegradation phenomenon occurring into the amorphous phase.

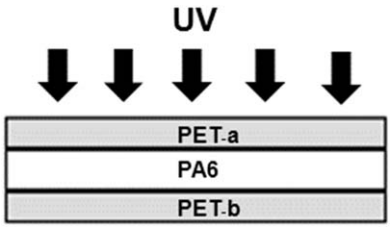

Figure 1. Multilayer film PET/PA6/PET exposed under UV radiations.

This kind of multilayer films may also be used in specific environment like the stratosphere (altitude ranging between 12 and 45 km). To investigate this multilayer performance upon a stratospheric exposure, a harsh environment has been selected. UV light selected was composed by UV with shorter wavelength presents at these altitudes, more energetic. Furthermore, ageing atmosphere was modified, with ozone gas addition and a temperature variation.

The aim of this study is identification and characterization of phenomena suffered by the multilayer film during its ageing into this simulated stratospheric environment. The influence of each parameters of ageing is studied to uncorrelate their impacts on the multilayer properties and on its different components.

EXPERIMENTAL

Materials

Multi-layers films used during this study are composed of PET-layers on theirs external sides, and PA 6 in its middle. A bicomponent thermosetting poly(urethane) (PU) adhesive fixed the different layers to each other. PET films were biaxially oriented films, produced in a two-step-stretching process: the first, in the travel direction, and the second, in the transverse direction. There had a nominal thickness of 15 μm. The PA-6 used was a biaxially oriented film produced by double bubble extrusion technology. It had thickness of 20 μm. The multilayer face exposed to the UV source is called (a) and the unexposed face is called (b) (Figure 1).

Ageing Conditions

Films were placed in a hermetic chamber, which reproduced stratospheric environment. Ageing parameters were a 20 km height conditions in temperate areas. All experiments were realized during 14 days. UV irradiation was achieved by a short arc Xenon lamp with filter. This system (lamp + filters) produces UV light with a cut-off at 270 nm. The UV radiations intensity (wavelength: 270 to 400 nm) reaching the sample surface is 56 W m^{-2}. The environment's temperature and pressure were fixed during the experiments. Irradiations were performed in air atmosphere, with a pressure fixed at 55 hPa. Air atmosphere was obtained pumping the ambient air to 55 hPa. Ozone gas (5 ppm, ozone concentration at 20 km) could be added in air using an additional monochromatic UV lamp (254 nm). Experiments are realized at a temperature of −55 °C (20 km height temperature) or +23 °C, during 14 days. An additional atmosphere condition was selected (at +23 °C) to investigate the oxygen presence impact on the multilayer evolution: nitrogen atmosphere. For the nitrogen atmosphere, after having pumped the atmosphere down to 10^{-1} mbar, the hermetic chamber was filled with nitrogen gas. This operation was reproduced three times. Finally, the atmosphere was pumped down to 55 hPa. After irradiation, samples were analyzed under air conditions.

Methods (Evaluation of Degradation)

Mechanical Properties Measurements. The mechanical properties were tested in a Instron 5569 machine operating with a 1 kN lead cell and a crosshead speed of 100 mm/min at room temperature. The sizes of the test specimen were 20 mm wide and 200 mm long with a 100 mm clamp separation. Tensile measurements were performed in traverse direction. The values of tensile strength and maximum elongation reported in this study correspond to averages calculated with the results obtained with at least five samples.

UV–Visible-Near Infrared Spectroscopy. UV–visible-near infrared spectra were recorded with a Perkin Elmer Lambda 900 UV–vis-NIR spectrometer associated with a 150 mm diameter integrating sphere in air. The transmission measurements were performed for each sample. The calibration curve was done with a diffuser Spectralon SRS-99-010 standard.

Fourier Transformed Infra-Red Analysis (FTIR) with an ATR Accessory. Films were analyzed by FTIR spectroscopy using a Equinox_55 Bruker spectrometer in the 400–4000 cm^{-1} range, with a resolution of 4 cm^{-1}. An attenuated total reflectance (ATR) accessory was used to quantify the surface layers degradation. The FTIR-ATR technique allowed investigating the first micrometer of the multilayer surfaces. The carboxyl end-groups index was used to characterize the degree of degradation of the PET layers. It has been defined as the ration of the ═OH vibration of the carboxylic acid endgroup absorption (peak at 3290 cm^{-1}) and the C═H absorption (peak at 2970 cm^{-1}).[19]

Differential Scanning Calorimetry (DSC). DSC measurements were carried out with a TA instrument (2920 CE). Films were analyzed in nonhermetically sealed aluminum pans. The sample weight was ranging from 5 to 10 mg. Thermograms were recorded at a heating rate of 10 °C/min in temperature range from −50 to +300 °C, under a dry helium gas purge at a flow rate of 110 mL min^{-1}. High purity indium and mercury were used for temperature and enthalpy calibration.

The melting temperature was taken at the maximum of the endothermic peak and the enthalpy variation calculated from the peak area. Normally, we evaluated the degree of crystallinity of PET and PA6 films, using eq. (1):

$$X_c = \Delta H_{f,\mathrm{net}} / \Delta H_\mathrm{o} \quad (1)$$

where ΔH_o is the heat of fusion of an ideal 100% crystalline, $\Delta H_{f,\mathrm{net}} = \Delta H_f - \Delta H_c$ is the net heat of fusion with ΔH_f being the heat of fusion, and ΔH_c is the heat of crystallization. Due to the presence of an endothermic peak caused by water desorption, cold crystallization regions are masked. Because of this, the PET and PA-6 degree of crystallinity cannot be calculated. In this work, we focused on the heat of fusion.

Dynamic Dielectric Spectroscopy. To determine the molecular mobility, measurements of the complex dielectric permittivity

$$\varepsilon^*(F) = \varepsilon'(F) - i\varepsilon''(F) \quad (2)$$

were carried out with a Novocontrol Broadband Dielectric Spectrometer (BDS4000), in the frequency range of 10^{-2}–10^{6} Hz.

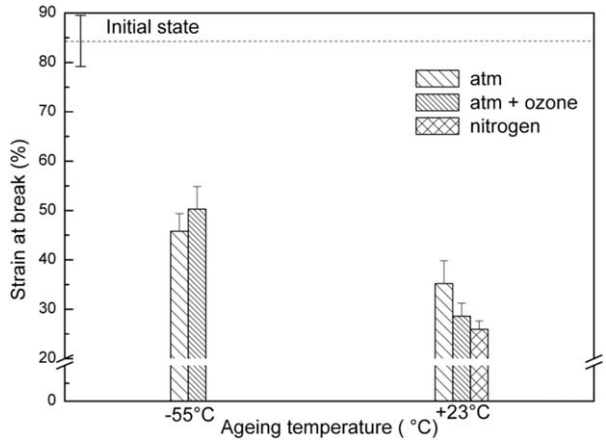

Figure 2. Evolution of the strain at break function of ageing parameters.

Experiments were performed isothermally from −150 to +150 °C by steps of 5 °C. The temperature in the cryostat was controlled with a stability of ±0.5 °C by a cold nitrogen gas stream, heated by a Quatro temperature controller. The samples were placed between gold-plated stainless steel electrodes (Ø = 20 mm).

The experimental limit for the loss factor ε'' was about 10^{-4}.

The real ε' and imaginary ε'' parts of the relative complex permittivity ε^* were measured as a function of frequency F at a given temperature T. From each isothermal plot, the relaxation modes were described by the double-stretched Havriliak–Negami (HN) function

$$\varepsilon*(\omega)=\varepsilon_\infty+\frac{\varepsilon_s-\varepsilon_\infty}{[1+(i\omega\tau_{HN})^{\alpha_{HN}}]^{\beta_{HN}}} \quad (3)$$

where ω is the angular frequency ($\omega = 2\pi F$), ε_s and ε_∞ are the relaxed ($\omega = 0$) and unrelaxed ($\omega = \infty$) dielectric constants, τ_{HN} is the relaxation time of HN model. The exponents α_{HN} and β_{HN} characterize the width and the asymmetry of the relaxation time distribution, respectively. At each temperature, a value of τ_{HN} was found for the modes present in the frequency window. The relaxation diagrams were plotted representing the variations of $\log \tau_{HN}(1/T)$, which are expected to be linear in the case of Arrhenius dependences for the relaxation time [eq. (4)] and curved for Vogel-Tammann-Fulcher ones [eq. (5)], according to the following expressions:

$$\tau_{HN}(T)=\tau_0 \exp\left(\frac{E_a}{RT}\right) \quad (4)$$

$$\tau_{HN}(T)=\tau_{0v}\exp\left(\frac{1}{\alpha_f(T-T_\infty)}\right) \quad (5)$$

where τ_0 and τ_{0v} are the pre-exponential factors, E_a the activation energy, and R the ideal gas constant, α_f the thermal expansion coefficient of the free volume, and T_∞ is the critical temperature at which any mobility is frozen. We must take the fitting procedure into account because of the presence of very often incomplete peaks despite the extension of frequency window of more than 8 decades. As the temperature increases, the relaxation peaks shift to higher frequencies and sweep the frequency window with different speeds, characteristic of the relaxation energy of each mode.

The fittings were performed with the nonlinear last-squares standard procedure Winfit from Novocontrol, starting from different initial parameters.

RESULTS AND DISCUSSION

Mechanical Properties

The mechanical properties evolutions with the ageing conditions have been investigated. The stress and the strain at break, reported Figures 2 and 3, are compared with the pristine one. The Young's modulus, not affected, is not reported. It value is 3970 ± 30 MPa for an unexposed multilayer.

Stress and strain at break present a significant decrease after UV irradiation for all atmosphere conditions. This decrease is usually observed after UV exposition of different polymers.[3,19,20] In the case of PET films, this decrease is linked with a molecular mass reduction, consequence of chain scission reactions during ageing.[21] Moreover, an increase of the ageing temperature leads to a decrease of stress and strain at break. This confirms the temperature as an accelerator character during photo-degradation. Conversely, the ozone gas addition in the chamber's atmosphere causes weak modifications of the mechanical properties within the measurement uncertainty, whatever the ageing temperature. The limited quantity of ozone (5 ppm) does not lead to significant modifications.

Values obtained after the ageing in nitrogen atmosphere at 23 °C show a slight additional diminution of this both properties.

UV–Visible Spectroscopy

The thermo-optical properties of pristine and UV irradiated multilayers were measured by UV–vis-NIR spectroscopy. The UV–vis curves obtained in transmission are presented Figure 4(a). To facilitate the observation of evolutions, we have reported on Figure 4(b) the T-Ti spectrum, calculated by subtracting the unaged multilayer film UV transmission spectra to the multilayer films aged ones.

A shift of the UV cut-off through the higher wavelengths and a transmittance decrease at low wavelengths are observed. Above the limit indicated by a dotted line at 360 nm in the Figure 4(b), the transmittance decrease is more important after the N_2 atmosphere ageing than after the oxidative ageing. Under 360 nm, the

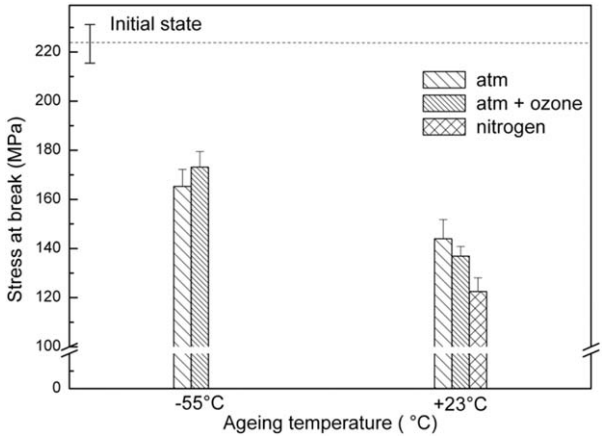

Figure 3. Evolution of the stress at break function of ageing parameters.

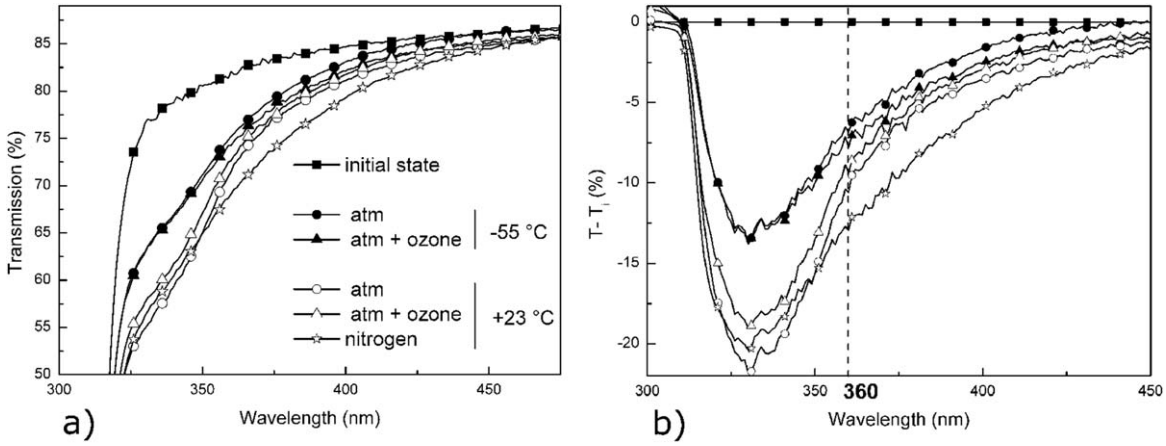

Figure 4. (a) UV–vis spectra of unexposed and different aged multilayer films (b) T-T$_i$ spectra representation.

transmittance decrease is more important for ageing in oxidative atmosphere, particularly after the 23 °C ageing.

Day and Wiles[16] had observed the technical properties evolution after UV radiations of PET films. They proposed reaction mechanisms of the photochemical degradation of PET with or without oxidative atmosphere.[16,17]

UV exposition causes scissions that creates radical. A nonoxidative ageing environment causes recombinations of radicals that leads to the creation of conjugate entities, like vinyl species, within the polymer.[16,22] These entities absorb wavelengths in the visible near UV region of the spectrum, responsible of the film yellowing.[12] On the contrary, an oxidative environment during irradiation leads to radical oxidations, which reduce recombinations. Therefore, creation of conjugated entities is lesser in oxidative environnement than in nonoxidative one. These mechanisms explain the higher absorption in the 350–450 nm region for the N_2 ageing spectrum.

Moreover, in presence of oxidative gas, photolysis leads to the creation of monohydroxy species which absorb UV around 340 nm.[17] This monohydroxy species creation can explain the additional decrease from 320 and 380 nm observed on the spectra of ageing in an oxidizing atmosphere. This reaction is more important in 23 °C than in low temperature.

FTIR Analysis

To investigate more precisely the possible impact of photodegradation on PET surface layers, FTIR-ATR studies have been performed. Only results of irradiated face (PET-a) are presented, no change has been observed on the rear surface. Photodegradation occurs mainly on the layer face exposed to UV irradiation, due to the slight UV penetration.[23]

Typical spectra of unexposed and exposed multilayers are represented Figure 5, focused in the modified carboxyl end-groups zone (2400–4000 cm^{-1}).

An optical density increase in the characteristic area is observed after the UV irradiation. The carboxyl end-groups index (Figure 6) shows an increase of carboxyl creation after UV irradiation, reflecting the PET-a degradation.

This carboxyl end-groups index increase is typical of the PET photo-degradation.[16,24] Day and Wiles have shown that the carboxyl end-groups are formed mainly via a Norrish type II photo rearrangement reaction. This reaction occurs independently of the ageing atmosphere. Additional formation is possible in oxidative atmosphere, via a Norrish type I cleavage reaction.[17] During this study, an increase of the ageing temperature causes a carboxyl end-groups index increase. The ageing atmosphere variation does not cause significant modification. The relative pressure, and thus

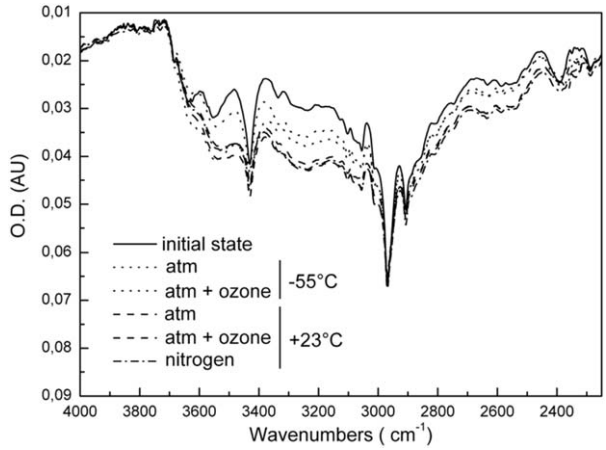

Figure 5. FTIR-ATR spectra of unexposed and different aged multilayer films.

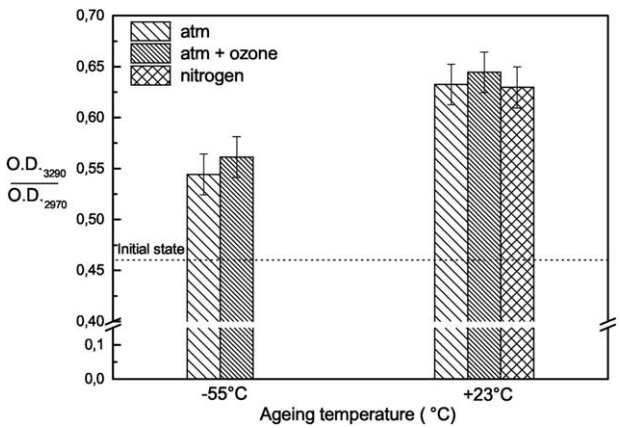

Figure 6. Evolution of carboxyl index function of ageing parameters.

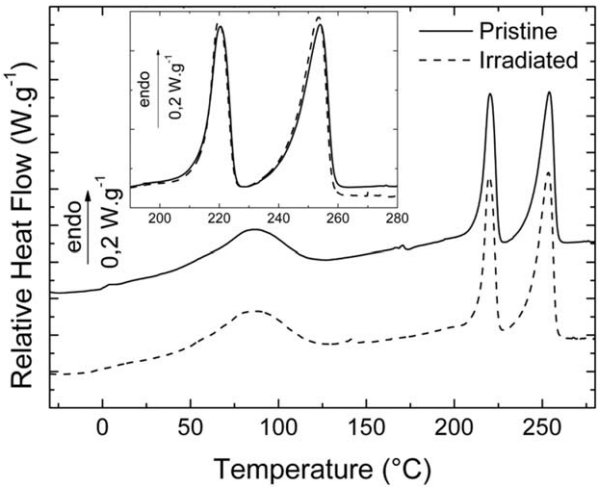

Figure 7. Typical DSC thermograms of unexposed and irradiated multilayers.

low numbers of oxygen molecules, does not cause sufficiently modifications via Norrish I reactions to be detected.

Several studies on PET films showed a weak increase of the carboxyl end-group index on the rear surface.[16,24] For ours multilayer films, the PET-a rear surface cannot be analyzed. The rear surface of the multilayers, corresponding to the rear surface of the PET-b film, is not modified during those ageing. In fact, the PET-b layer is protected from the photo-degradation by the two films, PET-a and PA-6, situated in front of him.

Thermal Analysis

Figure 7 presents the DSC thermograms obtained during the first heating run with a pristine multilayer and an irradiated one (ageing conditions: +23 °C, atm [55 mbar] + O_3 [5 ppm]). Thermograms obtained after different ageing conditions are similar, only one is shown.

A broad endothermic peak is observed around 80 °C, and at higher temperature, two endothermic peaks (220 and 255 °C). The identification of these events and their attribution to the different layers constituting the multilayer have been realized in a previous work.[18] Because of the presence of water desorption that masks the glass transition and the cold crystallization regions, only the crystalline melting zones have been investigated. Table I assesses the PET and PA-6 melting properties for unexposed and aged films.

Exposures of 14 days do not change significantly the heat of fusion and the melting temperature of PET and PA-6 films constituting the multilayer. It indicates that the crystalline phases of the various elements constituting the multilayer film are few or not affected by these ageing.

Fechine *et al.*,[25] studying PET films degradation, showed a little change (−3 °C) in melting temperature during a 43 days UV exposure, and no modification of crystallinity. Because the duration of our tests is short (14 days), modifications due to UV irradiation are not significant enough to induce modifications observable in DSC. Moreover, the observed PET signal is an average of the irradiated PET and the unirradiated PET film (PET-a and PET-b). According to the FTIR-ATR analysis, PET-b seems to be not modified during these ageing. This average diminishes the possible signal evolution caused by modifications.

The PA6 film, inside the multilayer, is protected by the PET films. It causes no sufficient modifications of its crystalline structure to be observed with DSC analysis.

Dynamical Dielectric Spectroscopy

The dielectric loss surface of an ageing multilayer film is shown in Figure 8 (ageing conditions: +23 °C, N_2 [55 mbar]). This 3D representation, characteristic of our multilayer films, reveals at low temperature two secondary relaxation modes γ and β, then at higher temperature two primary relaxation modes α_L and α_u. The identification of the different multilayer modes and their attribution to its different components has been discussed in a previous publication[18]: the dielectric relaxation modes of the multilayer correspond to the ones of the PA-6 internal layer. In fact, PA-6 dielectric spectrum has higher intensity than PET and adhesive ones in this temperature and frequency range, therefore masks the others signals.

As observed in this previous work, α_L is the only dielectric mode affected by UV exposition. The α_L mode is attributed to the PA-6 mobile amorphous phase (MAP) responsible for the glass transition observed by DSC measurements. Dielectric relation times τ_{HN}, extracted during the analysis of α_L relaxation mode using the HN function, have been reported in the Arrhenius diagrams (Figure 9).

For a same temperature analysis, α_L relaxation times are lower after UV irradiation. This shift is mainly pronounced with the +23 °C ageing in oxidative atmosphere (atm and atm + ozone). After the −55 °C ageing in oxidative atmosphere and the +23 °C ageing in nitrogen atmosphere, these evolutions are similar and low.

Table I. Melting Zone Parameters for the Unexposed and UV Exposed Multilayer Films

Ageing parameters		PA-6		PET	
		T_f^{PA6} (°C)	ΔH_f^{PA6} (J g^{-1})	T_f^{PET} (°C)	ΔH_f^{PET} (J g^{-1})
Initial state		220.6	53.4	254.2	43.4
−55 °C	Air (55 mbar)	220.5	48.1	255.0	41.7
	Air (55 mbar) + O_3 (5 ppm)	220.1	51.6	254.0	42.7
+23 °C	AAir (55 mbar)	220.2	53.9	253.6	44.7
	Air (55 mbar) + O_3 (5 ppm)	219.8	53.4	253.5	47.2
	N_2 (55 mbar)	220.0	51.3	253.4	44.5

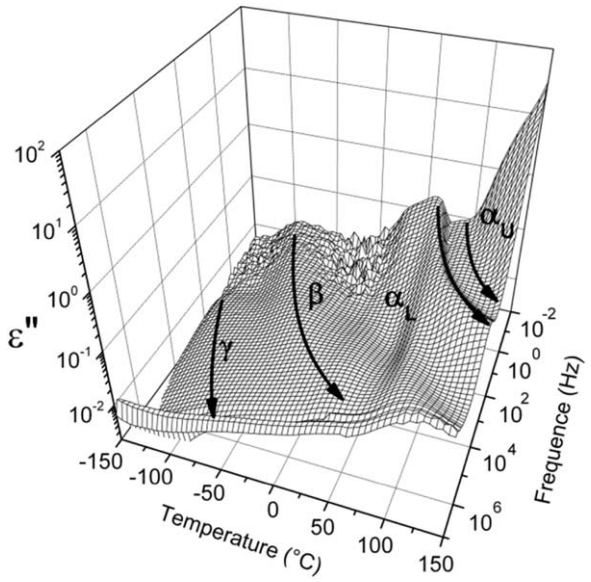

Figure 8. Dielectric loss surface of aged multilayer film obtained by DDS.

In our previous work, two assumptions have been made to explain the plasticizing effect observed on the α_L after UV irradiation: photolysis into the MAP create radicals, that are oxidized by oxidative gas, or water molecules combine with this radicals.[18] The irradiated multilayer in a non-oxidative environment (nitrogen) presents relaxation times close to the initial state, contrary to ageing in oxidative environment. These results are consistent with the first hypothesis: once the chain scissions are performed by photolysis into the MAP, in oxidative environment, radical oxidation occurs. This photo-oxidation causes a greater mobility of the macromolecules, resulting in this shift towards lower temperatures. Conversely, the lack of oxidative gas leads the radicals, created during the photolysis, to recombine each other or create conjugated entities. The molecular mobility is then low or no affected, as shown in Figure 9.

The oxidative gases responsible for this oxidation have to diffuse through the PET film to the PA-6 inner film. This diffusion is promoted by the temperature elevation.[26,27] During the −55 °C ageing, this gas diffusion is very low and the photo-oxidation is thus limited, resulting in a molecular mobility weakly affected, like in nitrogen environment.

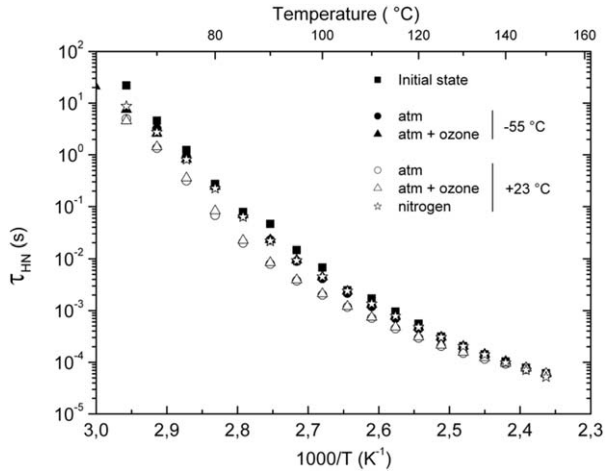

Figure 9. Relaxation times of multilayer before and after ageing.

CONCLUSIONS

A diminution of multilayer's mechanical properties at break and thermo-optical properties are observed when exposed to a stratospheric environment. These diminutions are the result of chain scissions resulting from photodegradation occurring during UV irradiation. The small addition of ozone (5 ppm), oxidative gas, does not cause additional evolution. A temperature elevation exacerbates the properties diminutions. UV irradiation of multilayer PET/PA-6/PET films makes similar evolution of technological properties to a single PET film. However, mechanical properties decreases are lower for the multilayer than those observed during the photodegradation of single PET film, due to the heterogeneous degradation of the different films constituting the multilayer.

Degradation is mainly located on the side of the multilayer exposed to UV radiation. However, the dynamic dielectric spectroscopy allowed studying the PA-6 layer, situated between two PET films. A plasticization of α_L during ageing is observed. Despite the protection of PET layers, degradation seems to occur in the PA-6 layer. This plasticization is due to the photo-oxidation of the PA-6, causing main chains scission, which causes a greater mobility of the macromolecules, resulting in this plasticization observed. This phenomenon is particularly observed after the ambient temperature ageing because of higher oxygen diffusion through PET films due to a higher thermal motion.

REFERENCES

1. Fechine, G. J. M.; Souto-Maior, R. M.; Rabello, M. S. *J. Appl. Polym. Sci.* **2007**, *104*, 51.
2. White, J. R.; Turnbull, A. *J. Mater. Sci.* **1994**, *29*, 584.
3. Rabello, M. S.; White, J. R. **1997**, *56*, 55.
4. Mailhot, B.; Gardette, J. L. *Macromolecules* **1992**, *25*, 4119.
5. Gijsman, P.; Meijers, G.; Vitarelli, G. *Polym. Degrad. Stab.* **1999**, *65*, 433.
6. Andrady, A. L.; Hamid, S. H.; Hu, X.; Torikai, A. *J. Photochem. Photobiol. B* **1998**, *46*, 96.
7. Rabek, J. F. Polymer Photodegradation. Mechanisms and Experimental Methods; Chapman and Hall: London, **1995**.
8. Scheirs, J.; Gardette, J. L. *Polym. Degrad. Stab.* **1997**, *56*, 339.
9. Wiles, D. M. *Polym. Eng. Sci.* **1973**, *13*, 74.
10. Allen, N. S.; Edge, M.; Mohammadian, M. *Polym. Degrad. Stab.* **1994**, *43*, 229.
11. Wang, W.; Taniguchi, A.; Fukuhara, M.; Okada, T. *J. Appl. Polym. Sci.* **1999**, *74*, 306.
12. Edge, M.; Allen, N. S.; Wiles, R.; McDonald, W.; Mortlock, S. V. *Polymer (Guildf)* **1995**, *36*, 227.

13. Fechine, G. J. M.; Christensen, P. A.; Egerton, T. A.; White, J. R. *Polym. Degrad. Stab.* **2009**, *94*, 234.
14. Edge, M.; Hayes, M.; Mohammadian, M.; Allen, N. S.; Jewitt, T. S.; Brems, K.; Jones, K. *Polym. Degrad. Stab.* **1991**, *32*, 131.
15. Gardette, J. L.; Colin, A.; Trivis, S.; German, S.; Therias, S. *Polym. Degrad. Stab.* **2014**, *103*, 35.
16. Day, M.; Wiles, D. M. *J. Appl. Polym. Sci.* **1972**, *16*, 191.
17. Day, M.; Wiles, D. M. *J. Appl. Polym. Sci.* **1972**, *16*, 203.
18. Lewandowski, S.; Rejsek-Riba, V.; Bernès, A.; Perraud, S.; Lacabanne, C. *J. Appl. Polym. Sci.* **2013**, *129*, 3.
19. Day, M.; Wiles, D. M. *J. Appl. Polym. Sci.* **1972**, *16*, 175.
20. Al-Madfa, H.; Mohamed, Z.; Kassem, M. E. *Polym. Degrad. Stab.* **1998**, *62*, 105.
21. Fechine, G. J. M.; Rabello, M. S.; Souto-Maior, R. M. *Polym. Degrad. Stab.* **2002**, *75*, 153.
22. Marcotte, F. B.; Campbell, D.; Cleaveland, J. A.; Turner, D. T. *J. Polym. Sci. Part A-1 Polym. Chem.* **1967**, *5*, 481.
23. Eickmeier, A.; Bahners, T.; Schollmeyer, E. *J. Appl. Phys.* **1991**, *70*, 5221.
24. Fechine, G. J. M.; Rabello, M. S.; Maior, R. M. S.; Catalani, L. H. *Polymer (Guildf)* **2004**, *45*, 2303).
25. Fechine, G. J. M.; Souto-Maior, R. M.; Rabello, M. S. *J. Mater. Sci.* **2002**, *37*, 4979.
26. Auras, R.; Harte, B.; Selke, S. *J. Appl. Polym. Sci.* **2004**, *92*, 1790.
27. Michaels, A. S.; Vieth, W. R.; Barrie, J. A. *J. Appl. Phys.* **1963**, *34*, 13.